RSC Advances

ROYAL SOCIETY OF CHEMISTRY

www.rsc.org/advances

Synthesis and physical properties of tris(dialkylamino)cyclopropenium bistriflamide ionic liquids

Kelvin J. Walst, Ruhamah Yunis, Paul M. Bayley, Douglas R. MacFarlane, Callum J. Ward, Ruomeng Wang and Owen J. Curnow

An investigation of symmetry (D_{3h}, C_{3h}, C_{2v} and C_s) and alkyl chain length (6–60 alkyl carbon atoms) effects on the physical properties of peralkylated triaminocyclopropenium bistriflamide salts.

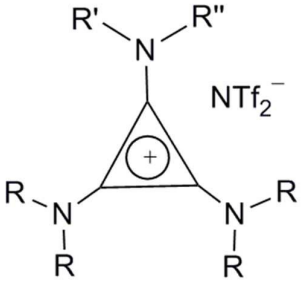

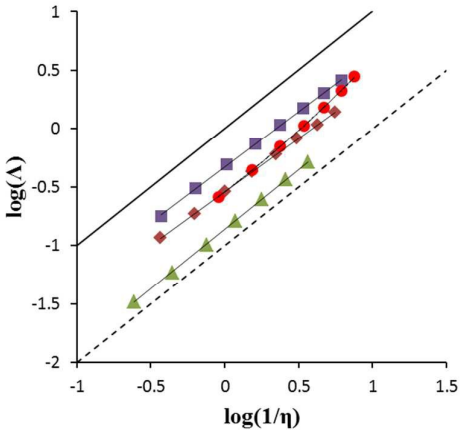

Journal Name

RSCPublishing

ARTICLE

Synthesis and physical properties of tris(dialkylamino)cyclopropenium bistriflamide ionic liquids

Cite this: DOI: 10.1039/x0xx00000x

Received ooth January 2012,
Accepted ooth January 2012

DOI: 10.1039/x0xx00000x

www.rsc.org/

Kelvin J. Walst,[a] Ruhamah Yunis,[a] Paul M. Bayley,[b] Douglas R. MacFarlane,[b] Callum J. Ward,[a] Ruomeng Wang[a] and Owen J. Curnow*[a]

The synthesis and properties of 23 tris(dialkylamino)cyclopropenium (TDAC) cations with the bistriflamide anion, NTf_2^-, are described. D_{3h}- and C_{3h}-symmetric cations ($[C_3(NR_2)_3]NTf_2$ (R = Me, Et, Pr, Bu, Pent, Hex, Dec) and $[C_3(NRMe)_3]NTf_2$ (R = Et, Bu, St), respectively) were synthesised by reaction of C_3Cl_5H with the corresponding amine. Reaction of alkoxydiaminocyclopropenium salts ($[C_3(NMe_2)_2(OMe)]^+$ and $[C_3(NEt_2)_2(OMe)]^+$) with amines led to two series of C_{2v}-symmetric salts ($[C_3(NMe_2)_2(NR_2)]NTf_2$ (R = Et, Pr, Bu, Hex) and $[C_3(NEt_2)_2(NR_2)]NTf_2$ (R = Me, Bu, Hex), respectively) and two series of C_s-symmetric salts ($[C_3(NMe_2)_2(NRMe)]NTf_2$ (R = Et, Pr, Bu, Hex) and $[C_3(NEt_2)_2(NRMe)]NTf_2$ (R = Bu, Hex), respectively). In addition to characterisation by NMR, mass spectrometry and microanalysis, the salts were characterised by DSC, TGA, density, viscosity, conductivity and miscibility/solubility studies. Along with molecular weight, symmetry plays a significant role in determining melting points and viscosity, whereas density was found to depend only on molecular weight. Methyl groups were found to significantly decrease thermal stability, while increasing the size of the other alkyl groups was found to increase stability; this increase in stability is contrary to observations with other classes of ionic liquids and indicates an associative decomposition mechanism. Walden plots indicated that these are "good ionic liquids" but that significant ion-pairing occurs when at least two alkyl chains of size C_6 or larger are present. Diffusion coefficients of $[C_3(NBu_2)_3]NTf_2$ revealed a relatively small loss conductivity due to ion correlations. The chemical stability of $[C_3(NEt_2)_3]NTf2$ to various reagents (acid, base, redox) was investigated at 25 °C and 60 °C. Cyclic voltammetry indicated a relatively small electrochemical window of 3.6 V (due to a relatively low oxidation potential of 1.2 V). The X-ray structures of $[C_3(NMe_2)_3]NTf_2$ and $[C_3(NPr_2)_3]NTf_2$ are reported.

1. Introduction

Ionic liquids (ILs) have undergone a rapid development over the past 15 years, particularly as many of these materials are now available and some are used on industrial scales.[1] The great attraction of these liquids arises from their general properties of almost zero vapour pressure, low flammability, ease of tunability, excellent solubilising properties and potential for efficient recycling. For these reasons, they are frequently considered as green alternatives to classical organic solvents.[2] Consequently, there are now a large number of applications, as detailed in several books on the subject.[3] Currently, there are five major cation-based classes of ILs (pyrrolidinium, imidazolium, pyridinium, phosphonium and ammonium) with the guanidinium[4,5] salts also being under recent investigation; the imidazolium, pyridinium and guanidinium families are notable in that the positive charge is delocalised and this reduces cation-anion interactions. Cyclopropenium salts, $[C_3R_3]X$, although known since the synthesis of $[C_3Ph_3]^+$ in 1957,[6] have not been investigated as ILs. The main reason for this is likely to be an expected lack of stability due to the strained three-membered ring. However, this instability is offset in the case of the triaminocyclopropenium (TAC) salts (R = NR'_2) due to the additional stability imparted by π donation from the three amino groups to the C_3 ring. TAC salts have been known for more than 40 years,[7] and have been recently reviewed by Komatsu and Kitagawa as well as Bandar and Lambert.[8,9] However, there have been essentially no investigations of their properties as ILs: Gompper and Schönafinger[10] reported the isolation of $[C_3(NMe_2)(N^iPr_2)_2]ClO_4$ and $[C_3(N^iPr_2)_3]ClO_4$ as red oils (although we isolated the former as a light brown solid[11] and the chloride hydrate of the latter as a colourless solid[12]) while

Wilcox and Breslow reported a melting point of 37.5–38.5 °C for $[C_3(NEt_2)_3]ClO_4$.[13] Some salts have reported melting points greater than 100 °C: Yoshida and Tawara reported melting points of 146 °C (dec) and 270 °C (dec) for the piperidine and morpholine perchlorate analogues, respectively,[7] while some mono- and di-amino-substituted cyclopropenium systems have also been found to have melting points greater than 100 °C.[14]

Compared to ammonium, phosphonium, and guanidinium cations, TAC cations have a greater delocalisation of the positive charge. Compared to the imidazolium, pyridinium and triazonium cations, they have reduced hydrogen bond donor capabilities due to a lack of aromatic C–H groups. Furthermore, it has been shown that these cations have a high-lying non-bonding HOMO that gives particularly weak cation-anion interactions.[15] A number of reports indicate that the TAC cation consequently has unusual properties as a result of these weak ionic interactions: Weiss and co-workers have prepared iodide-iodoacetylene and iodide-iodoarene adducts with "isolated" anions.[16] Similarly, we were able to isolate a discrete dichloride hexahydrate cube, $[Cl_2(H_2O)_6]^{2-}$, in which the solid state structure is essentially the same as the calculated gas-phase structure.[12]

This paper reports on the IL properties of tris(dialkylamino)cyclopropenium (TDAC) cations using the hydrophobic bistriflamide ($[N(SO_2CF_3)_2]^-$, NTf_2^-) counterion. Preliminary aspects of this work have been communuicated.[17,18]

2. Results and Discussion

2.1 Synthesis

TDAC salts were first prepared by reaction of tetrachlorocyclopropene with secondary amines,[7] and more recently by reaction with pentachlorocyclopropane.[17–19] These routes (Scheme 1) provide the D_{3h}- and C_{3h}-symmetric cations $[C_3(NR_2)_3]^+$ (**1**) and $[C_3(NRR')_3]^+$ (**2**), respectively, as the chloride salts. In a significant improvement for the synthesis of **1a**, we found that this salt can be prepared using 40% aqueous NMe_2H rather than the highly-volatile pure amine. Treatment of the chloride salts with aqueous $LiNTf_2$ readily provides the corresponding bistriflamide salts (**3** and **4**, respectively) which can be extracted into an organic solvent such as chloroform or dichloromethane. Earlier, we communicated the syntheses and some properties of $[C_3(NR_2)_3]NTf_2$ salts for R = Me, Et, Pr and Bu (**3a**–**d**) as well as the salt $[C_3(NBuMe)_3]NTf_2$ (**4a**).[1] Here we additionally include the related syntheses for R = Pent, Hex and Dec (**3e**–**g**) as well as $[C_3(NEtMe)_3]NTf_2$ (**4a**) and $[C_3(NStMe)_3]NTf_2$ (**4c**, St = $C_{18}H_{37}$). In some cases, the intermediate chloride salts were isolated and the properties of these materials will be described elsewhere.

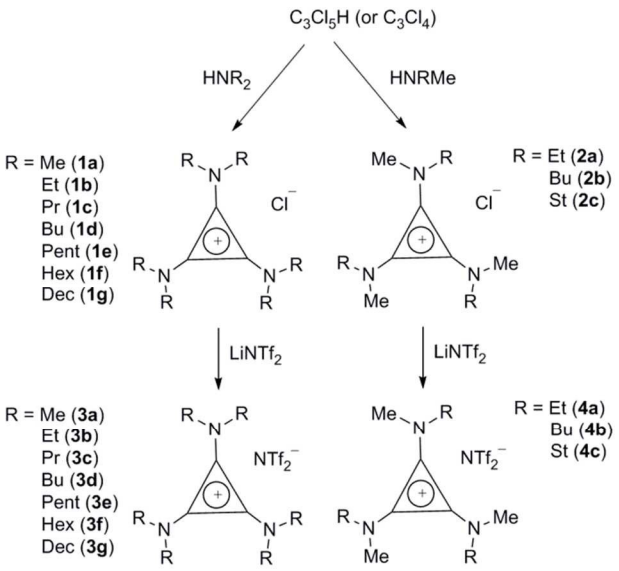

Scheme 1 Synthesis of D_{3h}- and C_{3h}-symmetric TDAC salts.

It is notable, in the case of the small amines $HNMe_2$ and HNEtMe, that significant amounts of the corresponding ring-opened allyldiamidinium cations $[HC_3(NMe_2)_4]^+$ (**5a**) and $[HC_3(NEtMe)_4]^+$ (**5b**), respectively, are formed (Scheme 2). These can be separated from the TDAC salts by addition of acid to convert the allyldiamidinium cations to the corresponding diamidinium dications $[H_2C_3(NMe_2)_4]^{2+}$ (**6a**) and $[H_2C_3(NEtMe)_4]^{2+}$ (**6b**), respectively, which are much more water soluble and are, therefore, not extracted into the organic phase. $[HC_3(NMe_2)_4]^+$ and $[HC_3(N^tBuH)_4]^+$ have been reported previously[19,20] and we will be describing the bistriflamide salts of these interesting cations in due course.

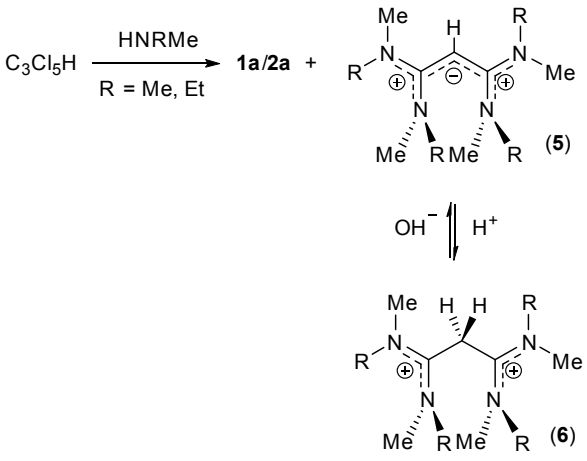

Scheme 2 Formation of allyldiamidinium and diamidinium cations.

If the secondary amine is bulky, such as $HNiPr_2$ or $HN(C_6H_{11})_2$, then its reaction with C_3Cl_5H or C_3Cl_4 gives the corresponding diaminochlorocyclopropenium cation $[C_3(NR_2)_2Cl]^+$ which can then be treated with a smaller secondary amine to provide a limited range of cations with C_{2v} and C_s symmetry: $[C_3(NR_2)_2(NR'_2)]^+$ and $[C_3(NR_2)_2(NR'R'')]^+$,

respectively, in which R is bulky and NR′R″ is reasonably small.[10,21] Due to the limited versatility of this route, we developed a route via reaction of secondary amines with the alkoxydiaminocyclopropenium cations $[C_3(NMe_2)_2(OMe)]^+$ (**7**) and $[C_3(NEt_2)_2(OMe)]^+$ (**8**) (Scheme 3). These are readily prepared in two steps: hydrolysis in hot aqueous base of the TDAC cation gives the diaminocyclopropenone which is then alkylated with dimethylsulfate to provide **7** or **8** as the methylsulfate salt. Reaction with secondary amines to generate the TDAC cation generally occurs quite readily, in a few hours or less, at ambient temperature. As with the chloride salts above, addition of aqueous $LiNTf_2$ followed by extraction with an organic solvent allows one to isolate the bistriflamide salts. Scheme 3 illustrates the four series of ILs that were prepared in this way: Two C_{2v}-symmetric series, **9** and **11**, via **7** and **8**, respectively; and two C_s-symmetric series, **10** and **12**, similarly via **7** and **8**, respectively. When looking at trends within these four series, note that some higher-symmetry species will also belong to some these series, i.e., **1a** can be included in series **9** and **10**; **1b** in series **11**; and **11a** in series **12**. Similarly, **1a** can be considered part of the C_{3h} **4** series of cations.

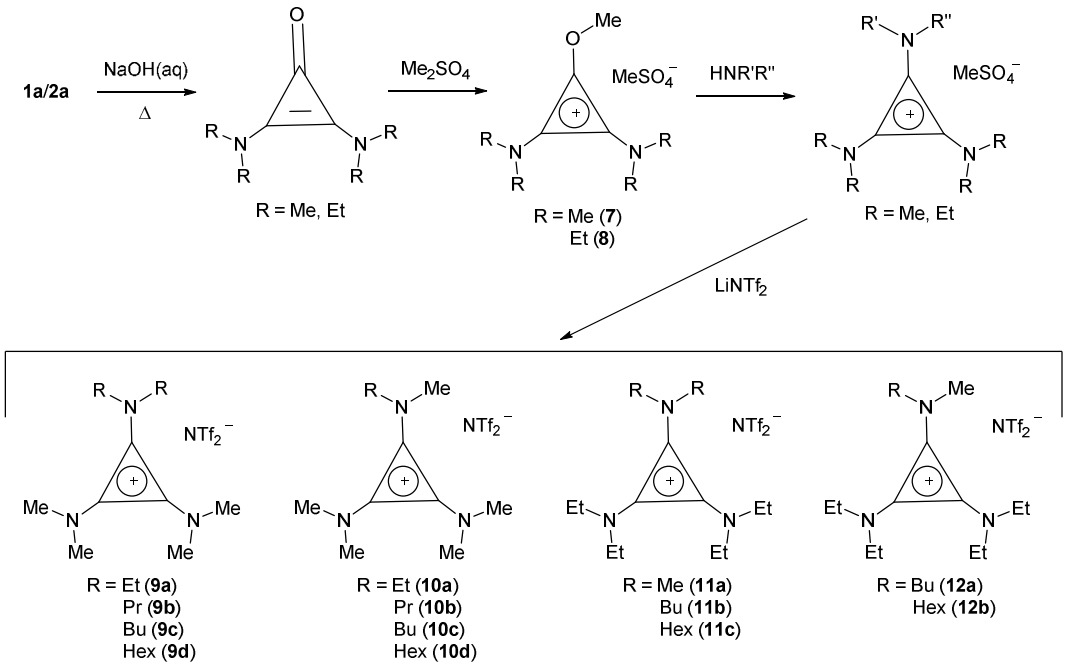

Scheme 3 Synthesis of C_{2v}- and C_s-symmetric TDAC salts.

In some cases, it proved to be more convenient, or significantly less expensive, to prepare class **10** compounds via the protic TAC IL $[C_3(NMe_2)_2(NRH)]NTf_2$ (**13**) (Scheme 4). Salts **13** were prepared by treatment of **7** with the appropriate primary amine. Deprotonation with *n*-BuLi gives the cyclopropenimine **14** which is readily alkylated, by reagents such as dimethylsulfate, to give salts **10** after anion exchange. Here, we provide details for the synthesis of **10a** and **10b** via **13a** and **13b**, respectively. In principle, this route can be used to generate a large range of TDAC ILs related to **9**–**12**. The properties of **13** and other related protic TAC ILs will be discussed elsewhere.

All new compounds were characterised by ^{1}H- and ^{13}C{^{1}H}-NMR spectroscopy as well as ES-MS and microanalysis. Chloride and water contents were determined for ILs prior to measurement of their physical properties; namely, DSC, TGA, viscosity, conductivity and density.

With respect to the NMR spectra, it should firstly be borne in mind that rotation about the exocyclic C–N bonds is fast on the NMR timescale; thus, a C_s-symmetric cation such as **10a** exhibits C_{2v} symmetry on the NMR timescale, and there is only one ^{1}H and ^{13}C-NMR signal for the NMe_2 groups. ^{1}H- and ^{13}C-NMR ranges are tabulated in the supplementary material. These are much as expected. Perhaps most noticeable is that the ^{13}C chemical shifts for the propyl C_β and C_ω atoms are ca. 10 and 3 ppm lower, respectively, than other alkyl groups (21–22 *vs* 29–32 ppm and 10.5–11 *vs* 13–15 ppm, respectively).

Journal Name

RSCPublishing

ARTICLE

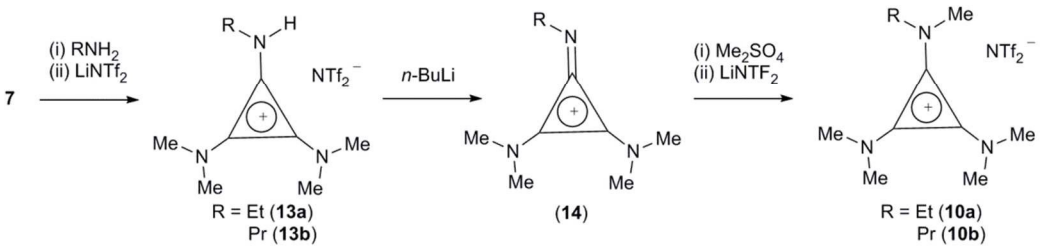

Scheme 4 Synthesis of C_s-symmetric TDAC salts via protic TAC salts.

2.2 DSC data

DSC data were collected at 10 °C/min and the results are given in Table 1. Not surprisingly, the only salt that is not an IL by definition is that with the smallest and most symmetric, D_{3h}, cation, **1a**, with a mp of 105 °C. A large number of factors are known to influence melting points: the various intermolecular forces (Coulombic, van der Waals, hydrogen-bonding etc.), conformational flexibility and the shape or symmetry of the species. Generally, it is found that ILs have high melting points for small ions in which Coulombic attractions dominate. They also have high melting points for large ions in which van der Waals interactions dominate. Reducing the symmetry or increasing the conformational flexibility of the side chains tends to reduce melting points since they reduce the factors that favour efficient packing in the solid state. Due to the large variety of symmetry classes presented here, it is most instructive to consider each class in turn.

Fig. 1 shows a plot of mp versus cation MW and carbon number for the D_{3h} class of cations. This shows a rapid drop in mp from **1a** as both size and conformational flexibility rapidly increase. Remarkably, the hexapropyl salt **3c** has a higher mp than the hexaethyl salt **3b**. It's not clear whether this is a result of chain flexibility issues or is related to the different ^{13}C-NMR chemical shifts mentioned earlier. The melting point appears to start increasing after the hexahexyl salt **3f**. However, with the exceptions of **3a** and **3c**, the changes are very small when you consider that on going from **3b** to **3f** there are an additional 24 CH_2 groups while on going from **3f** to **3g** there are a further 24 CH_2 groups.

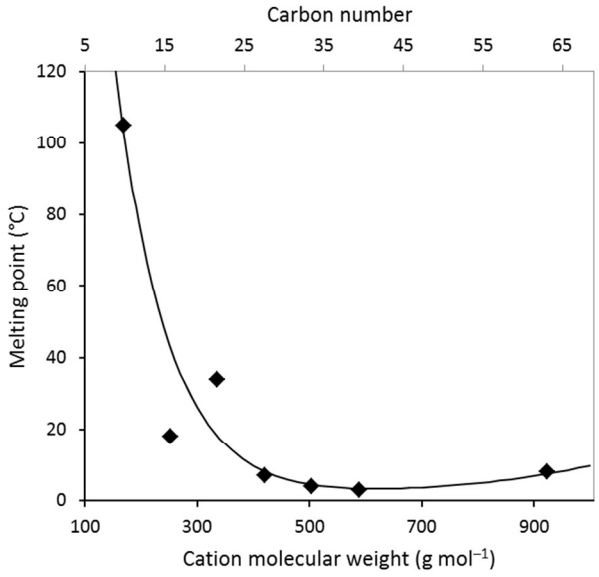

Fig. 1 Melting points of the D_{3h}-symmetry classes (salts **3**). The line is indicative of the trend.

Fig. 2 Illustrates the melting point trends of three series: the $[C_3(NMe_2)_2(NR_2)]NTf_2$ series which has C_{2v} symmetry, other than **1a** which is D_{3h}; the $[C_3(NEt_2)_2(NR_2)]NTf_2$ series which has C_{2v} symmetry, other than **1b** which is D_{3h}; and the $[C_3(NMe_2)_2(NRMe)]NTf_2$ series which has C_s symmetry, other than **1a** which is D_{3h}. The D_{3h}-symmetric salts are indicated on the figure. The two C_{2v} series show a similar rate of decrease in mp with increasing cation size, but with the bis(diethylamino) (**11**) salts having lower melting points than the corresponding isomer of the bis(dimethylamino) (**9**) salt. This may be attributed to the **9** series having up to six conformationally-flexible alkyl groups whereas the **11** series has at the most two conformationally-flexible alkyl groups. Another way of looking at this would be to say that the **11** series has a greater degree of

branching from the rigid tris(dimethylamino)cyclopropenium core. Notable exceptions to the decreasing mp with MW are that **9b** has a higher mp than **9a**, perhaps for the same reason that **3c** has a higher mp than **3b**, and that **3b** has a higher mp than **11a**, probably due to the increase in symmetry. Interestingly, the C_s series **10** shows a rapid decrease in the mp as the length of the alkyl chain increases. We attribute this to a more rapid decrease in symmetry from the disc-like D_{3h}-symmetric **1a** to a shape in which one chain protrudes out of the disc's edge at an angle (approximately 60°) and increasingly disrupts the packing efficiency.

Table 1 DSC (10 °C/min) and TGA data for bistriflamide salts

Salt	T_g /°C	$T_{S\text{-}S}$ /°C	T_m /°C	T_d at 1 °C min^{-1} /°C	T_d at 10 °C min^{-1} /°C
$[C_3(NMe_2)_3]NTf_2$ (**3a**)	–	45, 65, 83	105	309	339
$[C_3(NEt_2)_3]NTf_2$ (**3b**)	–86	–34, 1	18	349	393
$[C_3(NPr_2)_3]NTf_2$ (**3c**)	–72	–2	34	364	409
$[C_3(NBu_2)_3]NTf_2$ (**3d**)	–75	–	7	351	403
$[C_3(NPe_2)_3]NTf_2$ (**3e**)	–73	–	4	343	395
$[C_3(NHex_2)_3]NTf_2$ (**3f**)	–71	–	3	346	406
$[C_3(NDec_2)_3]NTf_2$ (**3g**)	–	–	8	349	401
$[C_3(NEtMe)_3]NTf_2$ (**4a**)	–	2	7	275	366
$[C_3(NBuMe)_3]NTf_2$ (**4b**)	–81	–	–	349	398
$[C_3(NStMe)_3]NTf_2$ (**4c**)	–	38, 48	65	338	384
$[C_3(NMe_2)_2(NEt_2)]NTf_2$ (**9a**)	–	27	44	232	334
$[C_3(NMe_2)_2(NPr_2)]$ NTf_2 (**9b**)	–	–	52	243	317
$[C_3(NMe_2)_2(NBu_2)]NTf_2$ (**9c**)	–42	–	36	250	314
$[C_3(NMe_2)_2(NHex_2)]NTf_2$ (**9d**)	–48	–	21	295	348
$[C_3(NMe_2)_2(NEtMe)]NTf_2$ (**10a**)	–	6, 32	63	211	315
$[C_3(NMe_2)_2(NPrMe)]NTf_2$ (**10b**)	–	–	20	247	291
$[C_3(NMe_2)_2(NBuMe)]NTf_2$ (**10c**)	–83	–	6	274	321
$[C_3(NMe_2)_2(NHexMe)]NTf_2$ (**10d**)	–	–	–14	264	295
$[C_3(NEt_2)_2(NMe_2)]NTf_2$ (**11a**)	–	–38, –31	17	340	379
$[C_3(NEt_2)_2(NBu_2)]NTf_2$ (**11b**)	–86	–	–4	355	403
$[C_3(NEt_2)_2(NHex_2)]NTf_2$ (**11c**)	–81	–	–	356	396
$[C_3(NEt_2)_2(NBuMe)]NTf_2$ (**12a**)	–89	–	–	341	384
$[C_3(NEt_2)_2(NHexMe)]NTf_2$ (**12b**)	–86	–	–	351	398

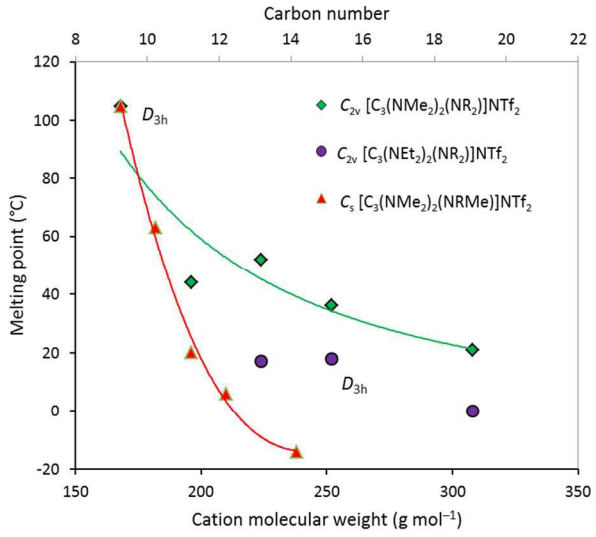

Fig. 2 Melting points of the C_{2v} (salts **9** and **11**) and C_s (salts **10**) symmetry classes. The lines are only indicative of the trends.

For the C_{3h} series of salts **4**, **4a** has a surprisingly low mp of 7 °C. This can be compared to its isomer **10c** which has essentially the same mp (6 °C) despite having much lower symmetry. This may be due to greater "branching" in **4a** or be related to the low mps observed for **3b** and **9a** relative to the salts next to them in their respective series; these ILs also have multiple ethyl groups. Salt **4b** is a liquid at ambient temperature, unfortunately, we were unable to observe a mp. Salt **4c** contains three long C_{18} chains and consequently has a high mp of 65 °C. This salt can be compared to **3g** with a mp of only 8 °C despite a slightly larger MW (884 *versus* 924 g mol^{-1}) and higher D_{3h} symmetry. In this case, the higher mp of **4c** can be attributed to fewer branching.

As might be expected for cations with four ethyl groups and C_s symmetry, salts **12a** and **12b** are liquids at ambient temperature. However, we were unable to obtain mps for these ILs.

2.2 Thermal decomposition

Thermal decomposition data were collected at both 1 °C min^{-1} and 10 °C min^{-1} and are given in Table 1. The major factor in determining the thermal decomposition onset temperature, T_d, is the number of methyl groups, and especially the number of dimethylamino groups. When none of the six alkyl groups are methyl groups (**3b**–**g**, **11b**,**c**), T_d is relatively invariant and there is no obvious trend with the size of the alkyl groups: at 1 °C

min^{-1}, T_d ranges 343–364 °C, while at 10 °C min^{-1}, it ranges 393–409 °C. Fig. 3 illustrates the trends for the 1 °C data only and further discussion focuses on this data. The most stable IL is the hexapropyl salt **3c**. The introduction of one methyl group, **12a** and **12b**, lowers T_d slightly to 341 and 351 °C, respectively. A second methyl group, in **11a**, again lowers T_d slightly (340 °C). As the number of methyl groups increases to three, **4a**–**c**, a dependence on the length of the non-methyl groups becomes apparent: the short ethyl groups in **4a** gives very low T_d values, 275 °C, while the longer C_4 and C_{18} chains in **4b** and **4c**, respectively, appear to provide enough steric protection to give relatively high T_d values, 349 °C and 338 °C, respectively.

The presence of four or five methyl groups, **9a**–**d** and **10a**–**d**, respectively, not only significantly lowers T_d, but also dramatically increases the dependency on the alkyl chain length, with longer chains leading to greater stabilities. There is approximately a 50–60 °C increase in stability from **9a** to **9d** and **10a** to **10d**. This trend is contrary to what is observed with imidazolium chloride and bistriflamide salts in which a small decrease (ca. 20 °C) in stability is found on going from [C_1mim]NTf_2 to [C_4mim]NTf_2, with even longer chains having no noticeable further effect.[22,23] This reduction in stability with increasing chain length is also seen in piperidinium bistriflamide salts and has been attributed to increased stability of carbocation and carbon radicals when the alkyl chain length increases.[24] IL thermal stabilities have recently been reviewed by Stevens and coworkers.[25] Given that longer alkyl chains afford more steric protection, an S_N2 type of mechanism is suggested for the decomposition of TDAC bistriflamide salts, possibly a reverse Menshutkin-type of reaction to generate a cyclopropenimine intermediate.

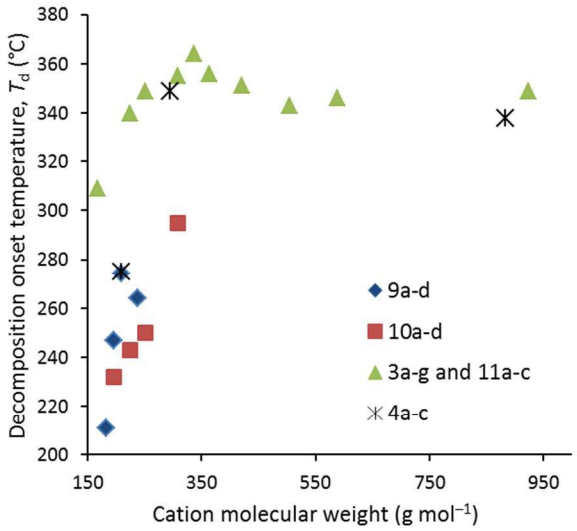

Fig. 3 T_d values of the tetramethyl (**9a–d**) and pentamethyl (**10a–d**) TDAC bistriflamide salts at 1 °C min^{-1}.

Somewhat curiously, the T_d value for the hexamethyl salt **3a** of 308 °C is higher than is found for all of the tetramethyl and pentamethyl salts. We have no good explanation for this observation. Possibly this is evidence of extended pi stacking, similar to the dicationic dimers that have been found in the halide salt **2a**,[26] as this would hinder attack by anions on the cation.

These T_ds are lower than most imidazolium and pyrrolidinium bistriflamide salts, but higher than pyridinium and phosphonium salts. For example, the T_d at 10 °C min^{-1} for [bmim]NTf_2 is 422 °C. Perhaps a better comparison is with the 2-Me isomer 1-propyl-2,3-dimethylimidazoium which has a T_d of 462 °C, well above the TDAC bistriflamide salts.[27] N,N-butylmethylpyrrolidinium bistriflamide has a T_d of 435 °C.[28]

For consideration of practical applications, isothermal decomposition profiles are desired. Workers have devised a number of methods to rapidly acquire this information. Measurement of the first-order rate constant for isothermal weight loss allows the determination of $t_{0.99}$ (the time for 1% of the sample to decompose). A plot of $t_{0.99}$ versus T generates an exponential decay curve from which $t_{0.99}$ can be calculated for any temperature. This is shown in Fig 4 for **3d** in both nitrogen and air atmospheres with $t_{0.99}(N_2) = (4.5 \times 10^{11})\exp(-0.044T)$ and $t_{0.99}(\text{air}) = (7.1 \times 10^{6})\exp(-0.022T)$, respectively. This can be compared to butylmethylpyrrolidinium bistriflamide for which $t_{0.99}(N_2) = (5.3 \times 10^{16})\exp(-0.059T)$.[28] The decomposition rates for TDAC salts appear to be less sensitive to temperature and this suggests a smaller contribution from entropy, perhaps indicating again an S_N2 mechanism. It is curious that the sensitivity of $t_{0.99}$ to temperature is less when in air (exponential factor of 0.022 compared to 0.044).

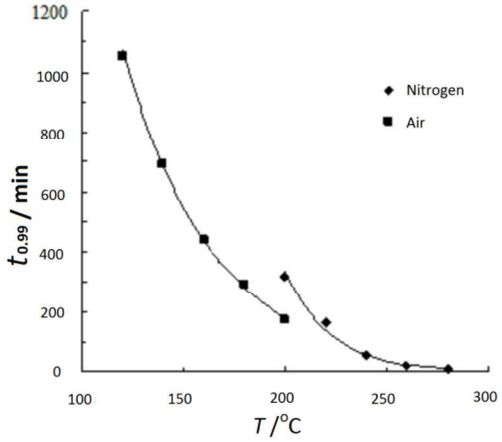

Fig. 4 $t_{0.99}$ *versus* isothermal temperature for **3d** under nitrogen and air atmospheres.

2.4 Density

Density data were determined from 20–90 °C where possible; the results for the 20 °C and 50 °C data are given in Table 2 and molar volumes are provided in the supplementary material. Unlike melting points, viscosities and conductivities, *vide infra*, densities for TDAC bistriflamide salts are independent of cation shape and depend only on the cation size (or mass). Fig. 5 shows a plot of densities at 20 °C *versus* the molecular weight (MW) of the cations for the bistriflamide salts as well as for

simple alkanes. Although it is frequently stated that densities decrease linearly with the number of CH_2 groups, clearly this is only true for short ranges of alkyl chain lengths. At long chain lengths, densities must approach that of very low density polyethylene (VLDPE), 0.88–0.915 g mL^{-1}, as the cation core and anions are increasingly diluted. The equations on Fig. 5 describe the fitted curves. These are made up of a volume for the permethyl salt **3a** of 528 $Å^3$, a factor of 27.7 $Å^3$ per CH_2 group added (n) to this core and a volume of 27.3 $Å^3$ per CH_2 group for alkanes (a volume of 52 $Å^3$ is used for the CH_4 core). These CH_2 volumes are in agreement with that obtained by Ye and Shreeve for ILs of 28 $Å^3$.[29] They also estimated a volume of 248 $Å^3$ for the bistriflamide anion in ILs which, therefore, gives us a volume for the $[C_3(NMe_2)_3]^+$ cation in ILs of 280 $Å^3$.

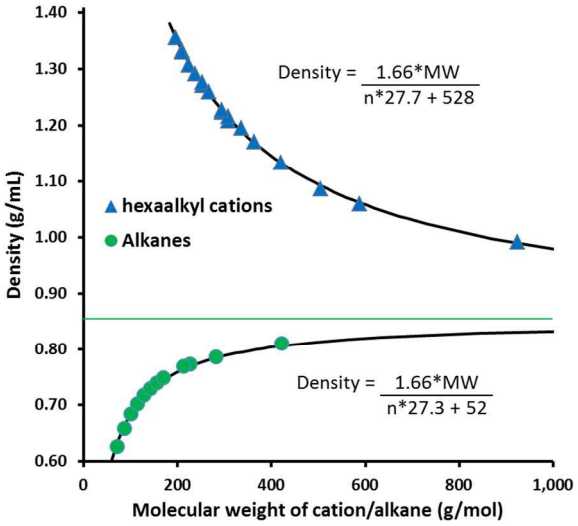

Fig. 5 Density at 20 °C versus the MW for TDAC bistriflamide salts and alkanes.

At 20 °C and n = ∞ , a density of 0.842 g mL^{-1} is calculated for TDAC bistriflamide salts and 0.853 g mL^{-1} for alkanes, i.e. effectively "liquid polyethylene". These are in quite good agreement and, interestingly, are only a little lower than is found in VLDPE, which presumably has some degree of crystallinity.

The densities of ILs have a linear dependency on temperature and can be well-fitted by the equation $\rho = a - bT$. Parameter a represents a theoretical density at 0 K. Pleasingly, a plot of a *versus* cation MW can also be fit (**3e**, **9b** and **10c** are possibly outliers, for reasons that will be apparent later) to a similar equation as the density data obtained at 20 °C (Supplementary, Fig. 1S). In this case, we calculate a volume for each CH_2 group at 0 K of 23 $Å^3$ while the volume of **3a** at 0 K was found to be 440 $Å^3$. This gives a "free volume" of 88 $Å^3$ for **3a** at 20 °C and 4.7 $Å^3$ per CH_2. Parameter a for "liquid polyethylene" (density at 0 K and n = ∞) is 1.012 g mL^{-1}.

Table 2 MW, cation hydrodynamic radius, and selected density, viscosity and conductivity data for TDAC bistriflamide ILs

	MW	r^+ at 20 °C[a]	Density		Viscosity		Conductivity	
	(g/mol)	(Å)	20 °C	50 °C	20 °C	50 °C	20 °C	50 °C
$[C_3(NEt_2)_3]NTf_2$ (**3b**)	532.61	4.74	1.277	1.251	94.7	27.5	1.387	3.681
$[C_3(NPr_2)_3]NTf_2$ (**3c**)	616.72	5.27	1.196	1.171	219.7	50.1	0.498	1.904
$[C_3(NBu_2)_3]NTf_2$ (**3d**)	700.89	5.71	1.134	1.111	230.4	55.2	0.428	1.535
$[C_3(NPe_2)_3]NTf_2$ (**3e**)	785.05	6.09	1.086	1.064	268.7	62.1	0.245	1.011
$[C_3(NHex_2)_3]NTf_2$ (**3f**)	869.21	6.42	1.059	1.037	273.0	65.3	0.141	0.508
$[C_3(NDec_2)_3]NTf_2$ (**3g**)	1205.86	7.51	0.991	0.970	407.6	84.6	0.027	0.131
$[C_3(NEtMe)_3]NTf_2$ (**4a**)	490.48	4.43	1.333	1.306	72.5	22.0	2.42	7.05
$[C_3(NBuMe)_3]NTf_2$ (**4b**)	574.64	5.02	1.224	1.199	101	26.8	0.939	2.825
$[C_3(NMe_2)_2(NEt_2)]NTf_2$ (**9a**)	476.45	4.31	–	–	–	25.1	–	5.15
$[C_3(NMe_2)_2(NPr_2)]$ NTf_2 (**9b**)	504.51	4.53	–	1.287	–	28.9	–	5.09
$[C_3(NMe_2)_2(NBu_2)]NTf_2$ (**9c**)	532.56	4.74	1.272	1.244	117.5	28.6	1.23	4.50
$[C_3(NMe_2)_2(NHex_2)]NTf_2$ (**9d**)	588.67	5.10	1.209	1.184	–	42.3	0.29	1.41
$[C_3(NMe_2)_2(NPrMe)]NTf_2$ (**10b**)	476.45	4.31	1.356	1.328	72.5	20.0	2.71	8.30
$[C_3(NMe_2)_2(NBuMe)]NTf_2$ (**10c**)	490.48	4.43	1.331	1.303	76.1	21.9	2.36	7.23
$[C_3(NMe_2)_2(NHexMe)]NTf_2$ (**10d**)	518.53	4.64	1.292	1.266	94.0	24.7	1.31	4.83
$[C_3(NEt_2)_2(NMe_2)]NTf_2$ (**11a**)	504.51	4.53	1.308	1.282	83.6	24.7	1.572	4.106
$[C_3(NEt_2)_2(NBu_2)]NTf_2$ (**11b**)	588.67	5.10	1.216	1.191	125.7	32.7	0.850	2.532
$[C_3(NEt_2)_2(NHex_2)]NTf_2$ (**11c**)	644.78	5.42	1.171	1.147	182.1	44.2	–	–
$[C_3(NEt_2)_2(NBuMe)]NTf_2$ (**12a**)	546.59	4.84	1.260	1.235	106.2	29.7	1.225	3.346
$[C_3(NEt_2)_2(NHexMe)]NTf_2$ (**12b**)	574.64	5.02	1.228	1.203	101.8	28.3	1.176	3.690

[a] Based on density data, see supplementary material for this calculation.

Journal Name

RSCPublishing

ARTICLE

Density parameter b represents the temperature dependency of the density. This parameter is rarely commented on, however, we find that this parameter is also well-fitted (again with the exceptions of **3e**, **9b** and **10c**) by an equation of the type used for the density at 20 °C and parameter a (Supplementary, Fig. 2S). This illustrates a decrease in temperature dependence with MW. Parameter b for "liquid polyethylene" is 5.82×10^{-4} g mL^{-1} K^{-1}. The combination of the equations for a and b allow us to derive a temperature-dependent equation for all TDAC bistriflamide salts (Eq. 1).

$$\text{Density} = 1.66*MW\left[\frac{1}{n*23 + 440} - \frac{T*10^{-4}}{n*4.0 + 78.8}\right] \quad \text{Eq. 1}$$

The thermal expansion coefficient α_p can be obtained from the slope of a plot of $\ln(\rho)$ versus T, i.e. $-[\partial\ln(\rho)/\partial T]_P = -c$.[30] Although α_p can vary with temperature,[28] and $\ln(\rho)$ versus T can be fit with quadratic or cubic functions, we have not done so due to the limited temperature range. The values of α_p vary from 0.653×10^{-3} K^{-1} for **9b** to 0.709×10^{-3} K^{-1} for **10c**, however, most values are in the range $0.680–0.705 \times 10^{-3}$ K^{-1}. These are similar to, but on the high end of, values found for other ILs: phosphonium ILs ($0.575–0.692 \times 10^{-3}$ K^{-1}),[31–34] imidazolium ILs (0.579–0.705),[28,35] and pyridinium ILs (0.530–0.543).[35] Our high values can probably be attributed to relatively higher MWs. A plot of α_p *versus* MW (Fig. 6) shows some dependency on MW, with α_p generally greater at higher MWs (as also found in imidazolium and phosphonium ILs),[31,32] although it is not as obvious as in the plots of a and b (Figs 1S and 2S, respectively). This plot also strongly suggests that **3e**, **9b** and **10c** are outliers (these ILs have also been indicated in Fig.s 1S and 2S where they are not so obviously outliers).

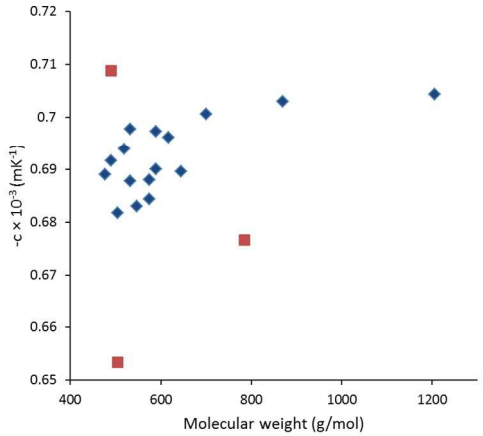

Fig. 6 Thermal expansion coefficient versus MW. ILs **3e**, **9b** and **10c** are indicated by red squares.

2.5 Viscosity

Viscosity data were collected from 20–90 °C where possible; the results for the 20 °C and 50 °C data are given in Table 2. As is to be expected, viscosity generally increases with MW, as shown in Fig. 7 for viscosity at 20 °C. Also shown on this plot is the 2-Me isomer of $[C_4mim]NTf_2$, $[C_3dmim]NTf_2$. The lower viscosity of $[C_4mim]NTf_2$ relative to $[C_3dmim]NTf_2$ has been attributed to a lower density and greater free volume in $[C_4mim]NTf_2$.[36] It is interesting then that the TDAC salts have viscosities that are much lower than the 2-Me imidazolium salts of similar MWs, despite having very similar densities.

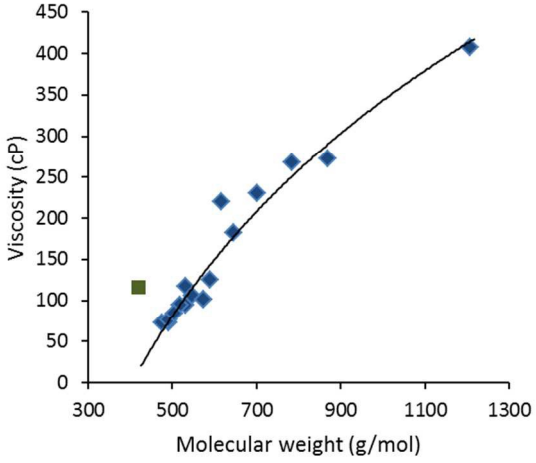

Fig. 7 Viscosity at 20 °C for TDAC bistriflamide salts and $[C_3dmim]NTf_2$ (green square). The trendline is indicative.

When the viscosity data is colour-coded by symmetry class, as shown in Fig. 8 for the data at 50 °C, some further trends become apparent. Relative to their MWs, the D_{3h} ILs **3b–g** and the C_{2v} ILs **9a–d** have similar viscosities (notably, **3b** and **9c** appear to be low and **3c** possibly high). On the other hand, the C_{2v} salts **11a–c** and the C_s salts **10b–d** have similarly lower viscosities. Interestingly, **3b** can also be considered part of the **11** series of salts $[C_3(NEt_2)_2NR_2]NTf_2$, in which R = Et, and its viscosity falls on this line rather than the upper line for the D_{3h}-symmetric salts **3**.

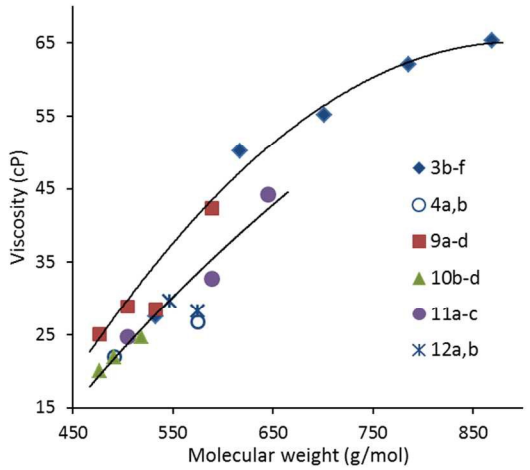

Fig. 8 Viscosity at 50 °C for TDAC bistriflamide salts. Trend lines are indicative.

Of the C_{3h}-symmetric salts, **4a** falls on the low viscosity line whereas **4b** lies even lower. The C_s-symmetric salt **12a** also lies on the low viscosity line, whereas **12b** lies below this line and even below **12a**.

Given the lack of symmetry effects on molar and, hence, free volumes. These differences in viscosities appear to due to a combination of conformational flexibility and symmetry: flexible chains facilitate the motion of molecules past each other and so lower viscosity, whereas higher symmetry increases viscosity, perhaps due to a greater degree of short range ordering. Of the "high" viscosity ILs, the D_{3h} salts **3** are highly symmetric whereas the slightly less-symmetric C_{2v} salts **9** have only two alkyl groups with conformational flexibility. Of the "low" viscosity IL series, The C_{2v} salts **11** have six conformationally-flexible alkyl groups while the C_s-symmetric salts **10** have only one flexible alkyl group but lowest symmetry. It appears, therefore, that low symmetry and conformationally-flexible alkyl groups lead to low viscosity. This possibly explains why **12b** has such a low viscosity for its MW: it has lowest symmetry and six flexible alkyl chains.

The viscosity data was fit to both the Arrhenius ($\eta = A\exp(E_a/RT)$) and Vogel-Fulcher-Tammann (VFT, Eq. 2) equations (also, $D = B/T_0$); these parameters are given in the supplementary material. There are not many obvious trends: E_a tends to increase with MW; The values of D, a measure of the deviation from Arrhenius behaviour, lie in the range 2.6–13.9 which is typical for "fragile" liquids.[37] A "fragility plot" of log(viscosity) versus T_g/T (supplementary material, Fig. 4S) similarly shows that these materials are typical of fragile ILs, although the C_{2v} salts **9c** and **9d** appear to be more fragile than the others due to higher T_g values. However, it is not obvious why this is the case.

$$\eta = \eta_0 \exp\left(\frac{B}{T - T_0}\right) \qquad \text{Eq. 2}$$

2.6 Conductivity

Conductivity data was collected from 20–90 °C where possible; results at 20 °C and 50 °C are given in Table 2. Fig. 9 illustrates the data at 50 °C for which a strong trend of decreasing conductivity with MW is observed. Unlike viscosity, there appears to be no obvious dependence of conductivity on the symmetry class of the cation. Given the normally expected strong relationship between viscosity and conductivity, this is quite surprising. A plot of log(conductivity) *versus* MW gives a reasonably straight line (Supplementary, Fig. 5S).

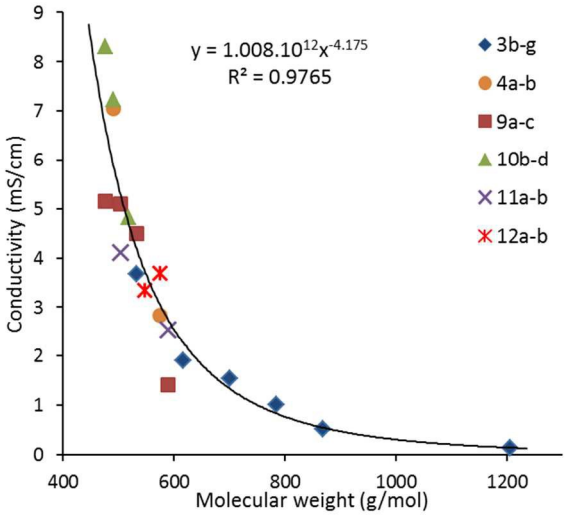

Fig. 9 Conductivity at 50 °C for TDAC bistriflamide salts.

2.7 Ionicity

Conductivity and viscosity are linked through Walden's rule: $\Lambda\eta$ = k (in which k is a temperature-dependent constant, the Walden product). A Walden plot, log(Λ) versus log($1/\eta$), can be used to investigate the ionicity of a conducting solution or liquid, with deviations from the ideal diagonal (represented by 1 M KCl(aq)) being ascribed to the formation of ion pairs or aggregates. The Walden plot for the ILs presented in this paper is given in Fig. 10. The majority of ILs fall in a narrow band with only a small deviation from ideal. These would thus be considered as "good ILs". Two lie further off this ideal line, namely **3f** and **9d**, both of which have dihexylamino groups. Furthest off the ideal line is **3g** which has three didecylamino groups. Salts **3e**–**g** and **9d** are shown separately in the supplementary material (Fig. 6S) for clarity. MacFarlane and co-workers have observed similar deviations in phosphonium chloride salts as the alkyl chain lengths have increased, and that was attributed to encapsulation of the chloride anion by the alkyl chains leading to ion pairs.[38] We suggest a similar explanation here in which two hexyl or decyl chains are able to encapsulate (or at least strongly interact via dispersion forces) the bistriflamide anion and thus form transient ion pairs. Interestingly, **9d** has the greatest slope in the Walden plot (1.12 *versus* 0.78–1.02 for the others), as well as noticeable deviation from linearity (the slope increases from 0.96 to 1.32 as T increases over the investigated temperature range), such that the ionicity is greatly increased at elevated temperatures and it

becomes similar in ionicity to the other ILs. To confirm that the anomalous Walden plot of **9d** is due to changes in ionicity, comparison of viscosity and conductivity with **3c**, which has a similar MW, is useful: At 303 K, **9d** has a lower viscosity than **3c** (110.3 versus 127.1 cP, respectively) but also a lower conductivity (0.53 versus 0.86 mS/cm, respectively). At 363 K, **9d** has a higher viscosity (13.2 *versus* 12.6 cP, respectively) and a correspondingly slightly lower conductivity (5.52 *versus* 5.64 mS/cm, respectively). This confirms that ion-pairing at lower temperatures has decreased both viscosity and conductivity in **9d** and suggests that the dihexyl-bistriflamide interactions get broken at higher temperatures to reduce the number of ion pairs. For **3f** and **3g**, on the other hand, presumably the bistriflamide anions can get passed from one diamino group to another. It is not clear why **3e**, with six pentyl groups, appears to have insufficient alkyl-bistriflamide interactions for ion pairing.

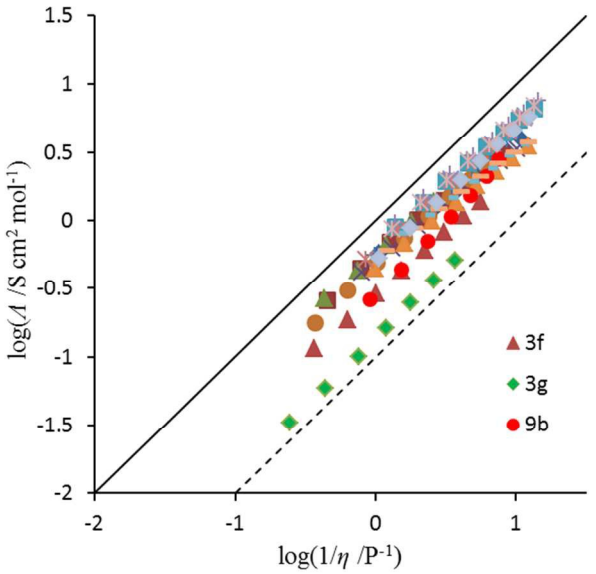

Fig. 10 Walden plot for TDAC bistriflamide salts.

MacFarlane developed an adjusted Walden plot to take into account the role of the ion sizes r^+ and r^-.[38] This plot and further discussion is presented in the supplementary material. The plot (supplementary, Fig. 7S) brings most of the salts to within likely uncertainties of the KCl line. Salts **3f**, **3g** and **9d**, however, are still distinctly below the line.

Ionicity was also investigated by measurement of the diffusion coefficients of **3d** at 20 °C: D^+ was found to be 3.17 × 10^{-12} m^2 s^{-1} and D^- is 5.62 × 10^{-12} m^2 s^{-1}. From the Nernst-Einstein equation, Λ_{NE} = 0.336 S cm^2 mol^{-1}. This compares to the measured molar conductivity, Λ_M, of 0.264 S cm^2 mol^{-1}. The ionicity can be defined as the ratio Λ_M/Λ_{NE}, which for **3d** is 0.79 (this can also be viewed as a 21% reduction in molar conductivity due to ion correlations). This is remarkably high compared to other bistriflamide-based ILs ([C_4mim]NTf_2 (Λ_M/Λ_{NE} = 0.61), [N_{4111}]NTf_2 (0.65), [C_4py]NTf_2 (0.63) and [C_4mpyr]NTf_2 (0.70)),[39] indicating possibly one of the highest values of ionicity ever observed in ILs at around room temperature. This result is even more surprising considering that Watanabe and co-workers showed that ionicity decreases with alkyl chain length for the imidazolium bistriflamide salts—to 0.53 for [C_8mim]NTf_2, which still has a significantly smaller MW than **3d** (475.5 *vs* 700.9 g mol^{-1}).[22a] They attributed this decrease to increasing dispersive forces.

Despite the high ionicity of **3d**, its relatively high MW means that the effective ionic concentration, C_{eff} (defined as molar concentration times Λ_M/Λ_{NE}), is still quite low at 1.28 × 10^{-3} mol cm^{-3}, compared to 2.9 × 10^{-3} mol cm^{-3} for [C_2mim]NTf_2 and 1.5 × 10^{-3} mol cm^{-3} for [C_8mim]NTf_2.[39a] Salt **10b**, the smallest RTIL reported here (MW = 476.5 g mol^{-1}), is likely to have an effective ionic concentration at 20 °C of 2.3–2.8 × 10^{-3} mol cm^{-3}. Watanabe and co-workers have described a number of correlations between C_{eff} and various physical properties, however the large difference in MW between **3d** and the salts discussed by them makes meaningful comparisons difficult at this stage.[39a,40]

The ionicity studies provide further evidence of the weak Coulombic interactions between TDAC cations and their anions. The NMR study has been limited at this stage due to limited NMR access time for these lengthy experiments, but will be pursued further in future work.

2.8 Miscibility and solubility

The miscibility and solubility properties of the salts were investigated at 25 °C. The results are given in Table 3 in order of increasing MW. All of the salts were found to be insoluble or immiscible in water but soluble or miscible in MeOH, EtOH, CH_2Cl_2 and EtOAc. The notable exceptions are the insolubility of **3a** in MeOH and EtOH (due to the small and highly-symmetric cation), as well as the insolubility of **4c** in MeOH, EtOH and EtOAc. Interestingly, **4c** was observed to swell in water but not dissolve. Clearly, the very long C_{18} chains have interesting effects on the properties of this salt.

In toluene, diethylether and hexane, miscibility/solubility was found to increase with MW. Much higher MWs are required for miscibility in hexane such that only **3g** is completely miscible in all proportions. For MWs of 575 to 869 g/mol, the ILs are partially miscible in hexane with the range of miscibility increasing with increasing MW. With partially-miscible samples, miscibility is always observed above a certain proportion of IL (say, above 50% IL), never within a broad intermediate range of proportions (such as 30–70%). This is because it is possible for organic solute molecules to find space in the IL without significantly disrupting the electrostatic attractions between ions whereas it is not possible for low-polarity solvents to separate the ions and create a solution of charged solute molecules. Again, **4c** was found to be very unlike **3f** and **3g** in that it is insoluble in hexane.

Toluene and diethylether exhibit quite similar solubility properties with partial miscibility being exhibited between approximately 476 and 645 g/mol. Symmetry effects and conformational flexibility appear to be very important in the exceptions to these trends. Greater symmetry decreases

solubility/miscibility whereas increased flexibility increases solubility/miscibility. Thus, (i) C_{2v}-symmetric **9a** is insoluble in toluene/diethylether whereas C_s-symmetric **10b**, of the same MW, is partially miscible, (ii) C_{2v}-symmetric **9b** is similarly insoluble in toluene and has reduced miscibility in diethylether compared to those of similar MW which have either reduced symmetry (**10c** and **10d**) or three or more flexible ethyl groups (**4a** and **11a**) compared to the two propyl groups of **9b** (notably, **9b** is also a solid at ambient temperature), (iii) D_{3h}-symmetric **3b** is insoluble in diethylether whereas all those with similar MW have lower symmetry and are at least partially miscible, (iv) **4b** (C_{3h}), **9d** (C_{2v} and four Me groups) and **3c** (D_{3h}) are insoluble in hexane whereas **12b** (C_s), **11b** and **11c** (both C_{2v} but with no Me groups) are partially miscible in hexane due to lower symmetry or increased flexibility. Salt **4c** is again an interesting exception: two immiscible liquid phases are formed in diethylether whereas it is, perhaps surprisingly, soluble in toluene.

Some solid samples were observed to form two immiscible liquid layers (**3a** with toluene, **9a** with Et_2O, **9b** with toluene and Et_2O, and **4c** with Et_2O), suggesting that at least a small amount of organic solvent must have dissolved into these ILs to break up the crystalline lattice. That **3a** should form an immiscible liquid under these conditions is particularly interesting given its high mp (105 °C). This suggests that the mp of this compound can be sharply decreased by the action of a second component.

Water is known to have a significant effect on the properties of ILs,[41] so we also measured water contents in some water-saturated systems: **3b** (5,140 ppm), **12b** (3,270 ppm) **3d** (3,500 ppm) and **3e** (2,340 ppm). A lot of data is available for other water-saturated bistriflamide salts.[23,41,42] Although there is significant variation in the reported values with some salts, there is a strong trend of decreasing water content with increasing MW as hydrophobicity increases, as shown in Fig 11 (data provided in supplementary material). Interestingly, water contents appear to have almost reached a lower limit of ca. 2,000 ppm with the TDAC bistriflamide salts due to their high MWs.

Table 3 Miscibility and solubility properties of TDAC bistriflamide salts at 25 °C[a]

Compound	MW	Water	MeOH/EtOH	CH_2Cl_2/EtOAc	Toluene	Et_2O	Hexane
$[C_3(NMe_2)_3]NTf_2$ (**3a**)	448	I	I	Y	N	I	I
$[C_3(NMe_2)_2(NEtMe)]NTf_2$ (**10a**)	462	I	Y	Y	I	I	I
$[C_3(NMe_2)_2(NEt_2)]NTf_2$ (**9a**)	476	I	Y	Y	I	N	I
$[C_3(NMe_2)_2(NPrMe)]NTf_2$ (**10b**)	476	N	Y	Y	≥ 50% IL	≥ 50% IL	N
$[C_3(NEtMe)_3]NTf_2$ (**4a**)	490	N	Y	Y	≥ 40% IL	≥ 50% IL	N
$[C_3(NMe_2)_2(NBuMe)]NTf_2$ (**10c**)	490	N	Y	Y	≥ 50% IL	≥ 40% IL	N
$[C_3(NMe_2)_2(NPr_2)]$ NTf_2 (**9b**)	505	I	Y	Y	N	≥ 71% IL	I
$[C_3(NEt_2)_2(NMe_2)]NTf_2$ (**11a**)	505	N	Y	Y	≥ 50% IL	≥ 50% IL	N
$[C_3(NMe_2)_2(NHexMe)]NTf_2$ (**10d**)	519	N	Y	Y	≥ 40% IL	≥ 25% IL	N
$[C_3(NMe_2)_2(NBu_2)]NTf_2$ (**9c**)	533	N	Y	Y	≥ 50% IL	≥ 33% IL	N
$[C_3(NEt_2)_3]NTf_2$ (**3b**)	533	N	Y	Y	≥ 50% IL	N	N
$[C_3(NEt_2)_2(NBuMe)]NTf_2$ (**12a**)	547	N	Y	Y	≥ 50% IL	≥ 50% IL	N
$[C_3(NBuMe)_3]NTf_2$ (**4b**)	575	N	Y	Y	≥ 33% IL	Y	N
$[C_3(NEt_2)_2(NHexMe)]NTf_2$ (**12b**)	575	N	Y	Y	≥ 50% IL	≥ 33% IL	≥ 77% IL
$[C_3(NMe_2)_2(NHex_2)]NTf_2$ (**9d**)	589	N	Y	Y	≥ 40% IL	Y	N
$[C_3(NEt_2)_2(NBu_2)]NTf_2$ (**11b**)	589	N	Y	Y	≥ 50% IL	≥ 33% IL	≥ 77% IL
$[C_3(NPr_2)_3]NTf_2$ (**3c**)	617	N	Y	Y	≥ 50% IL	≥ 33% IL	N
$[C_3(NEt_2)_2(NHex_2)]NTf_2$ (**11c**)	645	N	Y	Y	≥ 33% IL	Y	≥ 67% IL
$[C_3(NBu_2)_3]NTf_2$ (**3d**)	701	N	Y	Y	Y	Y	≥ 67% IL
$[C_3(NPe_2)_3]NTf_2$ (**3e**)	785	N	Y	Y	Y	Y	≥ 56% IL
$[C_3(NHex_2)_3]NTf_2$ (**3f**)	869	N	Y	Y	Y	Y	≥ 33% IL
$[C_3(NStMe)_3]NTf_2$ (**4c**)	1164	I	I	Y[b]	Y	N	I
$[C_3(NDec_2)_3]NTf_2$ (**3g**)	1206	N	Y	Y	Y	Y	Y

[a] I = insoluble; N = immiscible liquid; Y = soluble or miscible. [b] insoluble in EtOAc

Journal Name

RSCPublishing

ARTICLE

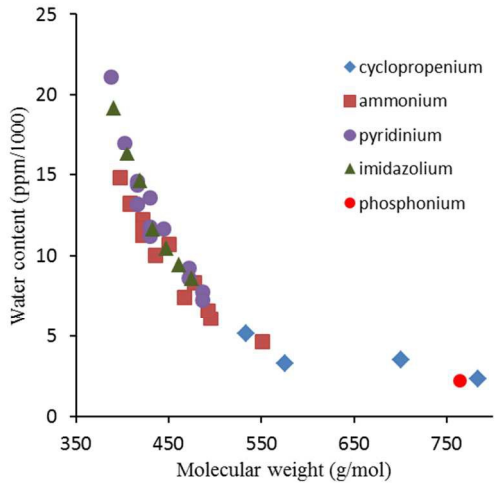

Fig. 11 Water contents of water-saturated alkyl-substituted bistriflamide ILs at 25 °C ("ammonium" includes pyrrolidinium and piperidinium).

2.9 Chemical stability

For the use of ILs in chemical processes, their stability under a variety of conditions needs to be examined. Tests based on those of Afonso *et al.*[43] were carried out on **3b** with one (or two) equivalents of reagent (acid (HCl), weak base and nucleophile (NH_3), strong base (NaOH), reducing agent ($NaBH_4$), oxidising agent ($NaIO_4$) and Grignard (EtMgI)) at room temperature and at 60 °C for 24 hours. Samples were then analysed by NMR. Salt **3b** was found to be stable under all of these conditions except for NaOH at 60 °C, with which it reacts to form diethylamine and the cyclopropenone. In the case of the Grignard reagent, although **3b** is stable, the Grignard is not active and presumably the lack of a suitable donor atom in the solvent causes the Grignard to become unstable with respect to $MgEt_2$ and MgI_2. Afonso and co-workers reported that [BMIM]Cl and $[NMe(n\text{-}C_8H_{17})_3]Cl$ are similarly unstable with NaOH at 60 °C, whereas the guanidinium salt $[C(NMe_2)(NHex_2)_2]Cl$ is stable in NaOH but unstable with 3 equivalents of $NaBH_4$ at 60 °C.[43] Noting the decreased thermal stability of the methylated TDAC salts **3a**, **9** and **10**, the chemical stability of these classes will be reported in due course. Nonetheless, these results suggest that TAC salts will be suitable solvents for a variety of reaction conditions.

2.10 Electrochemical stability

The electrochemical stability of an IL is an important property for any electrochemical application. It is the range of voltage over which the IL is electrochemically inert, i.e. neither oxidized nor reduced. The upper limit is the resistance of the IL to oxidation, and is generally determined by the more electron rich species: the anion. The lower limit is the resistance of the IL to reduction, and is generally, though not always, determined by the more electron poor species: the cation. The difference between these limits is the electrochemical window.

Cyclic voltammetry was carried out on a recrystallized sample of **3b** as a representative example of the structures synthesised in this work. This was dried under vacuum at 50 °C for 72 hours beforehand, due to water also having a negative effect on the size of the electrochemical window and the introduction of reduction peaks associated with the water. The final water content was 71 ppm.

The cyclic voltammogram is shown in Fig. 12, measured with a platinum working electrode and referenced to the Fc/Fc^+ redox couple. If a cut-off limit for current density of 1 mA cm^{-2} is used, then the oxidation limit of **3b** is 1.2 V. The negative peak on the return sweep around 1.2 V indicates that the oxidation process is to some extent reversible. Oxidation is usually ascribed to the anion, the more electron rich species, however, TFSA anions often resist oxidation up to 2.5 V, so in this case we are seeing oxidation of the cation. This agrees well with results reported by Johnson, who observed reversible oxidation of $[C_3(NMe_2)_3]^+$ in acetonitrile at 1.3 V.[44] This low oxidation limit further reinforces the electron rich nature of the TAC cation due to the extensive π donation from the amino substituents. The oxidation limit is lower than all the other common cation classes, Table 4, however, the potential reversibility of the process suggests possible applications of these materials in energy storage applications. We will explore this possibility in our future work.

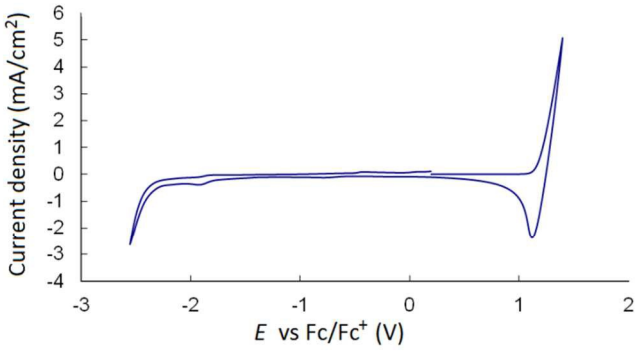

Fig. 12 Cyclic voltammogram of **3b**.

The reduction limit of **3b** was found to be –2.4 V. Reduction is usually ascribed to the cation, and this is the case here as well, as some bistriflamide ILs have been observed to have a reduction limit of less than –3.0 V. It is noted that

Johnson[44] observed reduction of $[C_3(NMe_2)_3]^+$ at less than –3.0 V, however, that was in solution. When comparisons are made to other classes of cations with bistriflamide anions, the reduction limit of **3b** is higher than $[C_4py]NTf_2$ by 1.0 V, but similar to $[P_{14,6,6,6}]NTf_2$, $[C_4mim]NTf_2$ and $[N_{6,2,2,2}]NTf_2$.[45,46]

The oxidation and reduction limits mean that **3b** has a moderate electrochemical window of 3.6 V, largely due to the low oxidation potential of TAC cations to the dication radical. The electrochemical window is smaller than imidazolium, phosphonium and ammonium ILs, but comparable to pyridinium ILs, which have a more positive reduction limit for the pyridinium cations.

Table 4 Electrochemical potentials of **3b** and selected ILs

IL	$E_{(red)}$ V vs Fc/Fc^+	$E_{(ox)}$ V vs Fc/Fc^+	EW V	ref
3b	–2.4	1.2	3.6	–
$[P_{14,6,6,6}]^+$	–2.7	2.5	5.2	45
$[C_4mim]^+$	–2.5	1.8	4.3	45
$[N_{6,2,2,2}]^+$	–2.6	2.1	4.7	45
$[C_4py]^+$	–1.4	2.4	3.8	46

2.11 X-ray crystallography

Crystals of **3a** and **3c** were investigated by X-ray diffraction studies. Salt **3a** packs in the $P2_1/c$ space group with three independent cations and anions in each unit cell. Each cation is sandwiched between two bistriflamide anions which are oriented in one of two ways: (mode A) with the N atom, two O and two F atoms near the cation, or (mode B) by two O atoms and four F atoms near the cation. One independent cation interacts via two mode A, one via two mode B and the other by one of each mode. The latter combination is shown in Fig 13. The C–C distances range 1.371(3)–1.382(4) Å with an average of 1.377 Å. The exocyclic C–N distances range 1.320(3)–1.328(3) Å with an average of 1.325 Å while the N–Me distances range 1.446(4)–1.458(3) Å with an average of 1.452 Å. At least 16 salts containing $[C_3(NMe_2)_3]^+$ have been crystallographically characterised and the distances found here for the bistriflamide salt are typical.[16,47]

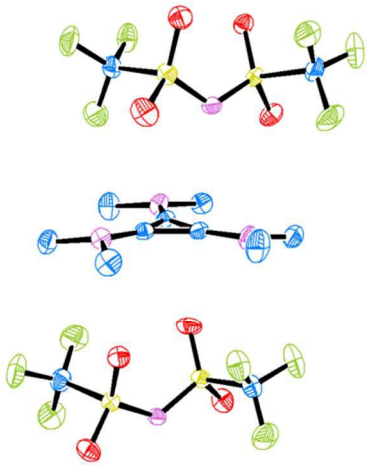

Fig. 13 ORTEP of **3a** illustrating one cation and the anions above (mode A) and below (mode B) the cation plane.

Salt **3c** packs in the I_2 space group with two independent cations and anions in the unit cell. Fig. 14 shows the two cations along with the bistriflamide anions above and below the ring. In each case, fewer anion atoms are in the vicinity of the cation coplanar atoms than is found in **3a**. This appears to be a combination of steric effects from protruding Pr groups as well as the presence of more anion-alkyl chain interactions. Both cations have adopted a conformation with four alkyl groups on one side and the other two on the other side. A mode A interaction occurs on the side with two alkyl groups, but with the anion displaced by the alkyl groups such that the amido atom lies over a $N(CH_2)_2$ group, rather than the C_3 ring as seen in **3a**. The four protruding alkyl groups on the other side of the cation force a mode B type of interaction in which the anion is displaced such that only one O and two F atoms are near the coplanar C_3N_3 atoms. The ring C–C bond distances are slightly longer and range 1.381(4)–1.389(4) Å with an average of 1.385 Å. The N–Pr distances are also slightly longer (average 1.329 Å) than the corresponding N–Me distances, whereas the exocyclic C–N bond distances are quite similar (an average of 1.466 Å). The CH_2–CH_2 distances in **3c** average 1.509 Å whereas the CH_2–CH_3 distances average 1.520 Å. The bistriflamide anions in both structures are found in the more stable trans configuration (C–S---S–C ranges 164.4(2)°–174.5(2)°).

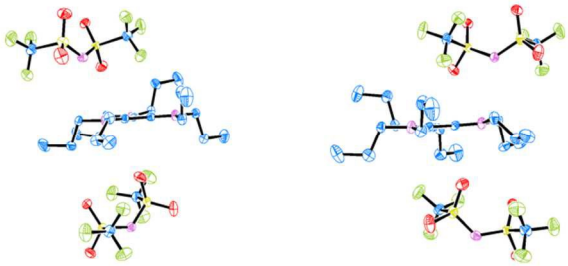

Fig. 14 ORTEP of **3c** illustrating the two cations and their anions (mode A above and mode B below the cation plane).

3. Conclusions

We have prepared a number of TDAC bistriflamide salts with a range of MWs and a variety of symmetry classes. The melting points can be nicely rationalised by consideration of MWs, symmetry and conformational flexibility. TGA studies found that dimethylamino (and ethylmethylamino) groups significantly decrease thermal stability while an increase in stability is found with increasing alkyl chain length when there are Me groups present. This indicates that steric factors, rather than electronic factors, control the rate of decomposition, and that the mechanism is S_N2. Density was found to be strongly dependent on MW and temperature, but not symmetry. Density fitting parameters a and b are strongly correlated with MW whereas the thermal expansion coefficient α_P was found to be

relatively poorly correlated, although similar in magnitude to other ILs. Viscosity similarly is highly MW dependent, but subtle differences occurs whereby higher symmetry increases viscosities and increased alkyl flexibility lowers viscosities. Somewhat surprisingly, conductivity does not appear to be obviously affected by these viscosity differences and is largely MW dependent. A Walden plot revealed that most of the ILs can be classified as "good ILs". Similarly, diffusion coefficient measurements confirmed that ion correlations are low, at least for short alkyl chains. Significant ion-pairing occurs when there are at least two alkyl chains of C_6 or longer. With only one dihexylamino group (**9d**), the ionicity was found to increase with increasing temperature. As is common with most bistriflamide salts, the TDAC salts are insoluble/immiscible in water but soluble/miscible in small polar organic solvents. Solubility/miscibility in non-polar solvents was found to be largely dependent on MW, but also subtly dependent on symmetry and conformational flexibility. Stability to common reagents (acid, base, redox) is very good with the exception of NaOH at elevated temperatures. Grignard reagents, however, appear to be unstable in these ILs. The addition of ether functional groups may be beneficial, as donor solvents are known to stabilise Grignard reagents. The electrochemical window was found to be quite small and similar to pyridinium salts, however, this is due to a low oxidation potential rather than a high reduction potential, so their use in reducing environments is still feasible while the reversibility of the oxidation process may be beneficial. The solid state structures of **3a** and **3c** further illustrate the steric protection afforded to the coplanar TAC atoms by addition of longer alkyl chains.

4. Experimental

All operations were performed using standard Schlenk techniques with a dinitrogen atmosphere in order to reduce exposure to water. ^{1}H-, ^{13}C{^{1}H}-NMR spectra were collected on a Varian Unity-300 operating at 300 and 75 MHz, respectively, an Agilent DD2-400MR operating at 400 and 100 MHz, respectively, or on a Varian INOVA-500 operating at 500 and 126 MHz, respectively, in $CDCl_3$, referenced to residual solvent peaks. Electrospray mass spectrometry was carried out on a Micromass LCT, with samples dissolved in acetonitrile. Water contents were determined by Karl Fischer titration using a Metrohm 831 KF coulometer. Chloride contents were determined using a AutolabEco Chemie, with associated GPES software, under a dinitrogen atmosphere. The electrodes were either a glassy carbon (3 mm diameter) or platinum (1 mm diameter) working electrode, a platinum wire counter electrode and a silver reference electrode. Mircoanalysis was performed by Campbell Microanalytical Laboratory, Dunedin. Pentachlorocyclopropane (Acros), dimethylsulfate, diethylamine (Merck), dipropylamine (Acros), dibutylamine (Koch-Light), dipentylamine, didecylamine, butylmethylamine, hexylmethylamine, stearylmethylamine, ethylamine, propylamine, and triethylamine (Sigma-Aldrich) were used as obtained commerically. $LiNTf_2$ (3M) was kindly provided by Prof. Ken Marsh. Ethylmethylamine was prepared by a modification of methods described by Lucier and Wawzonek.[48] The following salts were prepared by previously published methods: $[C_3(NMe_2)_3]NTf_2$ (**3a**),[17] $[C_3(NEt_2)_3]NTf_2$ (**3b**),[17] $[C_3(NPr_2)_3]NTf_2$ (**3c**),[17] $[C_3(NBu_2)_3]NTf_2$ (**3d**),[17] $[C_3(NBuMe)_3]NTf_2$ (**4b**),[17] $[C_3(NEt_2)_2NMe_2]NTf_2$ (**11a**),[18] $[C_3(NEt_2)_2NBu_2]NTf_2$ (**11b**),[18] $[C_3(NEt_2)_2NHex_2]NTf_2$ (**11c**),[18] $[C_3(NEt_2)_2NBuMe]NTf_2$ (**12a**)[18] and $[C_3(NEt_2)_2NHexMe]NTf_2$ (**12b**)[18].

Syntheses of the starting materials $[C_3(NMe_2)_3]Cl$ (**1a**), $C_3(NMe_2)_2O$ and $[C_3(NMe_2)_2(OMe)]MeSO_4$ (**7**) are provided in the supplementary material along with the syntheses and characterisation details of the TDAC salts: **1e**, **3e**, **1f**, **3f**, **1g**, **3g**, **4a**, **2c**, **4c**, **9a**, **9b**, **9c**, **9d**, **13a**, **10a**, **13b**, **10b**, **10c** and **10d**.

DSC was performed on a Perkin Elmer Q100: Samples of mass 5–20 mg were sealed in a vented aluminium pan and placed in the furnace with a 50 mL/min nitrogen stream; the temperature was raised at 10 °C/min. TGA data were collected on dried samples using a TA Instruments SDT Q600 at 10 °C/min after further drying at 100 °C for one hour in the instrument. Density measurements were carried out on an Anton Parr DMA 5000 instrument, an oscillating U-tube density meter, from 20 to 90 °C in 10 °C steps. Viscosities were measured on an Anton Parr AMVn falling-ball viscometer or a Brookfield-Wells cone-and-plate viscometer operating at 0.005–0.2 s^{-1} rotation speed range. Conductivity of **3e**, **3g** and **12b** were measured using a Schott LF4100+ probe and an impedance bridge conductivity meter. The instrument was calibrated with 0.1 mol L^{-1} KCl solution. All other conductivities were measured by AC impedance spectroscopy on a Solatron SI 1296 frequency response analyser, at ranges up to 0.01 Hz to 10 MHz. Measurements were carried out with a dip cell probe containing two platinum wires covered in glass. The resistance was identified using a Nyquist Plot, and conductivity then calculated using $\kappa = l/AR$, where l/A is the cell constant, which was determined using 0.01 mol L^{-1} KCl solution at 25 °C. All samples were measured from 20 °C (or above the melting point if solid) to 80 or 90 °C, and performed sealed or under a dinitrogen gas flow.

Solubility and miscibility studies were carried out by taking 0.5 mL of sample and adding step-wise 10 × 0.05 mL of solvent followed by 9 × 0.5 mL of solvent. After each addition of solvent the sample was mixed and allowed to equilibrate at 25 °C to determine whether the sample was miscible or immiscible. In the case of solid samples, a 0.1 g sample was taken and 2.5 mL of solvent was added and the sample was equilibrated at 25 °C. In some cases, the solid sample was observed to form two immiscible liquid layers. Water contents of water-saturated ILs were measured by Karl-Fischer titration after equilibration at 25 °C for 24 hours followed by centrifugation.

Chemical stability tests were conducted by placing a 250 mg sample with an equimolar amount of HCl (38%, aq), NH_3 (40%, aq, 2 equivalents), KOH, $NaBH_4$, $NaIO_4$ or EtMgI, and stirring at ambient temperature or at 60 °C. After 24 hours, ^{1}H-

NMR was used to assess whether any degradation of the cation had occurred.

Cyclic voltammetry was carried out using an Eco Chemie Autolab PGSTAT 302N potentiostat running GPES 4.9 software. A platinum working electrode (1.2 mm diameter), platinum wire secondary electrode and silver wire reference electrode were used. Recrystallized $[C_3(NEt_2)_3]$TFSA was dried under vacuum at 50 °C for 72 hours, which reduced water content to 71 ppm. Sample was degassed by bubbling with argon for 60 min before the experiment, and kept under an argon atmosphere for the experiments. Once the electrochemical window was measured, ferrocene was added to the IL as an internal reference.

X-ray crystallography: Single crystals of **3a** and **3c** formed in the neat liquid. A suitable crystal of each was selected and mounted on a SuperNova, Dual, Cu at zero, Atlas diffractometer. Using Olex2,[49] the structures were solved with the XS structure solution program[50] using Direct Methods and refined with the XL refinement package[50] using Least Squares minimisation. Crystal data and structure refinement and structural details are given in the supplementary material along with the atom numbering schemes.

Acknowledgements

Dr. Matthew Polson and Dr. Chris Fitchett for X-ray data collection and refinement.

Notes and references

[a] *Department of Chemistry, University of Canterbury, Private Bag 4800, Christchurch 8041, New Zealand. E-mail: owen.curnow@canterbury.ac.nz; Fax: +64 3 364 2110; Tel: +64 3 364 2819*

[b] *School of Chemistry, Monash University, Wellington Road, Clayton, Victoria 3800, Australia.*

† Electronic Supplementary Information (ESI) available: Synthesis and characterisation details of starting materials and TDAC salts; tables of typical ^{1}H- and ^{13}C-NMR chemical shift ranges, density data (with fit parameters), molar volumes, viscosity, viscosity fit parameters, conductivity, conductivity fit parameters, water contents of water-saturated bistriflamide ILs, crystallographic data for **3a** and **3c**, bond lengths and angles for **3a** and **3c**; Figures of density parameters *versus* MWs and atomic numbering schemes for **3a** and **3c**; a fragility plot; and an adjusted Walden plot with associated discussion. Crystallographic data in CIF format is available: CDCC 1055725 and 1055726. See DOI: 10.1039/b000000x/

1. N. V. Plechkova and K. R. Seddon, *Chem. Soc. Rev.*, 2008, **37**, 123.
2. For example: (a) *Ionic Liquids in Synthesis*, 2nd Ed, ed. P. Wasserscheid and T. Welton, Wiley-VCH, 2008; (b) *Ionic Liquids as Green Solvents: Progress and Prospects*, ed. R. D. Rogers and K. R. Seddon, *ACS Symp. Ser.*, vol. 856, American Chemical Society, Washington D.C., 2003; (d) *Green Solvents II: Properties and Applications of Ionic Liquids*, ed. A. Mohammad and Dr. Inamuddin, Springer Netherlands, 2012.
3. For example: *Ionic Liquids IIIB: Fundamentals, Progress, Challenges, and Opportunities – Transformations and Processes*, ed. R. D. Rogers and K. R. Seddon, *ACS Symp. Ser.*, vol. 902, American Chemical Society, Washington D.C., 2005; *Electrochemical Aspects of Ionic Liquids*, ed. H. Ohno, Wiley-Interscience, Hoboken, 2005.
4. See: (a) H. Kunkel and G. Maas, *Eur. J. Org. Chem.*, 2007, 3746 and references therein. (b) P. S. Kulkarni, L. C. Branco, J. G. Crespo, M. C. Nunes, A. Raymundo and C. A. M. Afonso, *Chem. Eur. J.*, 2007, **13**, 8478.
5. (a) W. Kantlehner, E. Haug, W. W. Mergen, P. Speh, T. Maier, J. J. Kapassakalidis and H.-J. Bräuner, *Synthesis*, 1983, 904. (b) W. Kantlehner, E. Haug, W. W. Mergen, P. Speh, J. J. Kapassakalidis, H.-J. Bräuner and H. Hagen, *Liebigs Ann. Chem.*, 1984, 108.
6. R. Breslow, *J. Am. Chem. Soc.*, 1957, **79**, 5318.
7. (a) Z. Yoshida and Y. Tawara, *J. Am. Chem. Soc.*, 1971, **93**, 2573; (b) Z. Yoshida, *Top. Curr. Chem.*, 1973, **40**, 47.
8. K. Komatsu and T. Kitagawa, *Chem. Rev.*, 2003, **103**, 1371.
9. J. S. Bandar and T. H. Lambert, *Synthesis*, 2013, **45**, 2485.
10. R. Gompper and K. Schönafinger, *Chem. Ber.*, 1979, **112**, 1514.
11. J. R. Butchard, O. J. Curnow, R. J. Pipal, W. T. Robinson and R. Shang, *J. Phys. Org. Chem.*, 2008, **21**, 127.
12. (a) J. R. Butchard, O. J. Curnow, D. J. Garrett and R. G. A. R. Maclagan, *Angew. Chem. Int. Ed*., 2006, **45**, 7550; (b) J. R. Butchard, O. J. Curnow, D. J. Garrett, R. G. A. R. Maclagan, E. Libowitzky, P. M. B. Piccoli and A. J. Schultz, *Dalton Trans.*, 2012, **41**, 11765.
13. C. Wilcox and R. Breslow, *Tetrahedron Lett.*, 1980, **21**, 3241.
14. (a) R. Weiss and C. Priesner, *Angew. Chem. Int. Ed. Engl.*, 1978, **17**, 445. (b) Y. Yagyu, N. Matsumura, H. Tanaka, Z. Maeda and H. Inoue, *J. Chem. Res. (S)*, 1995, 420.
15. R. Weiss and K. Schloter, *Tetrahedron Lett.*, 1975, 3491.
16. (a) R. Weiss, T. Brenner, F. Hampel and A. Wolski, *Angew. Chem. Int. Ed. Engl.*, 1995, **34**, 439. (b) R. Weiss, M. Rechinger, F. Hampel and A. Wolski, *Angew. Chem. Int. Ed. Engl.*, 1995, **34**, 441. (c) R. Weiss, O. Schwab and F. Hampel, *Chem. Eur. J.*, 1999, **5**, 968.
17. O. J. Curnow, D. R. MacFarlane and K. J. Walst, *Chem. Commun.*, 2011, **47**, 10248.
18. O. J. Curnow, M. T. Holmes, L. C. Ratten, K. J. Walst and R. Yunis, *RSC Advances*, 2012, **2**, 10794.
19. (a) M. J. Taylor, P. W. J. Surman and G. R.Clark, *J. Chem. Soc., Chem. Commun*., 1994, **21**, 2517; (b) G. R. Clark, P. W. J. Surman and M. J. Taylor, *J. Chem. Soc. Faraday Trans.*, 1995, **91**, 1523.
20. Z. Yoshida, H. Konishi, Y. Tawara, K. Nishikawa and H. Ogoshi, *Tetrahedron Lett.*, 1973, 2619.
21. (a) J. S. Bandar and T. H. Lambert, *J. Am Chem. Soc.*, 2012, **134**, 5552; (b) H. Heydt, P. Eisenbarth, K. Feith, K. Urgast, G. Maas and M. Regitz, *Israel J. Chem.*, 1986, **27**, 96; (c) H. Bruns, M. Patil, J. Carreras, A. Vazquez, W. Thiel, R. Goddard and M. Alcarazo, *Angew. Chem. Int. Ed.*, 2010, **49**, 3680; (d) R. Weiss, K. G. Wagner, C. Priesner and J. Macheleid, *J. Am. Chem. Soc.*, 1985, **107**, 4491; (e) R. Weiss and R. H. Lowack, *Bull. Soc. Chim. Belg.*, 1991, **100**, 483; (f) R. Gompper and K. Schönafinger, *Chem. Ber.*, 1979, **112**, 1535.
22. (a) H. Tokuda, K. Hayamizu, K. Ishii, M.. A. B. H. Susan and M. Watanabe, *J. Phys. Chem. B*, 2005, **109**, 6103. (b) J. G. Huddleston, A. E. Visser, W. M. Reichert, H. D. Willauer, G. A. Broker and R. D. Rogers, *Green Chem.*, 2001, **3**, 156.

23. J. G. Huddleston, A. E. Visser, W. M. Reichert, H. D. Willauer, G. A. Broker and R. D. Rogers, *Green Chem.*, 2001, **3**, 156.
24. M. Montanino, M. Carewska, F. Alessandrini, S. Passerini and G. B. Appetecchi, *Electrochim. Acta*, 2011, **57**, 153.
25. C. Maton, N. De Vos and C. V. Stevens, *Chem. Soc. Rev.*, 2013, **42**, 5963.
26. D. L. Crittenden, O. J. Curnow, C. D. Jayasinghe, M. I. J. Polson and A. J. Wallace, manuscript in preparation.
27. T. J. Wooster, K. M. Johanson, K. J. Fraser, D. R. MacFarlane and J. L. Scott, *Green Chem.*, 2006, **8**, 691.
28. M. Tariq, A. P. Serro, J. L. Mata, B. Saramago, J. M. S. S. Esperança, J. N. C. Lopes and L. P. N. Rebelo, *Fluid Phase Equilib.*, 2010, **294**, 131.
29. C. Ye and J. M. Shreeve, *J. Phys. Chem. A*, 2007, **111**, 1456.
30. Confusingly, a is frequently used in this equation for the slope, with b for the intercept, which is similar but contrary to the use of a and b in a plot of ρ *versus T*. Thus, we have used c and d here to eliminate this confusion.
31. G. Adamová, R. L. Gardas, L. P. N. Rebelo, A. J. Robertson and K. R. Seddon, *Dalton Trans.*, 2011, **40**, 12750.
32. G. Adamová, R. L. Gardas, M. Nieuwenhuyzen, A. V. Puga, L. P. N. Rebelo, A. J. Robertson and K. R. Seddon, *Dalton Trans.*, 2012, **41**, 8316.
33. M. Tariq, P. A. S. Forte, M. F. C. Gomes, J. N. C. Lopes and L. P. N. Rebelo, *J. Chem. Thermodyn.*, 2009, **41**, 790–798.
34. J. M. S. S. Esperança, H. J. R. Guedes, M. Blesic and L. P. N. Rebelo, *J. Chem. Eng. Data*, 2006, **51**, 237.
35. Z. Y. Gu and J. F. Brennecke, *J. Chem. Eng. Data*, 2002, **47**, 339.
36. Z. J. Chen and J.-M. Lee, *J. Phys. Chem. B*, 2014, **118**, 2712.
37. (a) C. A. Angell, J. *Non-Cryst. Solids*, 1991, **131–133**, 13; (b) C. A. Angell in *Molten Salts and Ionic Liquids: Never the Twain?* Ed. M. Gaune-Escard and K. R. Seddon, John Wiley & Sons, Hoboken, 2010, 1–24; (c) J.-P. Belieres and C. A. Angell, *J. Phys. Chem. B*, 2007, **111**, 4926.
38. D. R. MacFarlane, M. Forsyth, E. I. Izgorodina, A. P. Abbott, G. Annat and K. Fraser, *Phys. Chem. Chem. Phys.*, 2009, **11**, 4962.
39. (a) H. Tokuda, S. Tsuzuki, M. A. B. H. Susan, K. Hayamizu and M. Watanabe, *J. Phys. Chem. B*, 2006, **110**, 19593. (b) H. Tokuda, K. Hayamizu, K. Ishii, M. A. B. H. Susan and M. Watanabe, *J. Phys. Chem. B*, 2004, **108**, 16593. (c) H. Tokuda, K. Ishii, M. A. B. H. Susan, S. Tsuzuki, K. Hayamizu, and M. Watanabe, *J. Phys. Chem. B*, 2006, **110**, 2833. (d) H. Tokuda, K. Hayamizu, K. Ishii, M. A. B. H. Susan and M. Watanabe, *J. Phys. Chem. B*, 2005, **109**, 6103. (e) A. Noda, K. Hayamizu and M. Watanabe, *J. Phys. Chem. B*, 2001, **105**, 4603.
40. K. Ueno, H. Tokuda and M. Watanabe, *Phys. Chem. Chem. Phys.*, 2010, **12**, 1649.
41. K. R. Seddon, A. Stark and M.-J. Torres, *Pure Appl. Chem.*, 2000, **72**, 2275.
42. (a) K. Machanová, A. Boisset, Z. Sedláková, M. Anouti, M. Bendová, J. Jacquemin, *J. Chem. Eng. Data*, 2012, **57**, 2227; (b) M. G. Freire, C. M. S. S. Neves, K. Shimizu, C. E. S. Bernardes, I. M. Marrucho, J. A. P. Coutinho, J. N. C. Lopes and L. P. N. Rebelo, *J. Phys. Chem. B*, 2010, **114**, 15925; (c) K. Řehák, P. Morávek and M. Strejc, *Fluid Phase Equilib.*, 2012, **316**, 17; (d) J. Jacquemin P. Husson, A. A. H. Padua and V. Majer, *Green Chem.*, 2006, **8**, 172. (e) C. M. S. S. Neves, P. J. Carvalho, M. G. Freire, J. A. P. Coutinho, *J. Chem. Thermodynamics*, 2011, **43**, 948; (f) Y. Cao, Y. Chen, X. Wang and T. Mu, *RSc Advances*, 2014, **4**, 5169; (g) E. J. Gonzalez and E. A. Macedo, *Fluid Phase Equilib.*, 2014, **383**, 72; (h) M. G. Freire, P. J. Carvalho, R. L. Gardas, I. M. Marrucho, L. M. N. B. F. Santos and J. A. P. Coutinho, *J. Phys. Chem. B*, 2008, **112**, 1604 (i) M. G. Freire, C. M. S. S. Neves, P. J. Carvalho, R. L. Gardas, A. M. Fernandes, I. M. Marrucho, L. M. N. B. F. Santos and J. A. P. Coutinho, *J. Phys. Chem. B*, 2007, **111**, 13082; (j) J. Salminen, N. Papaiconomou, R. A. Kumara, J.-M. Lee, J. Kerr, J. Newmana and J. M. Prausnitz, *Fluid Phase Equilib.*, 2007, **261**, 421; (k) N. Papaiconomou, J. Salminen, J.-M. Lee and J. M. Prausnitz, *J. Chem. Eng. Data*, 2007, **52**, 833.
43. (a) P. S. Kulkarni, L. C. Branco, J. G Crespo, M. C. Nunes, A Raymundo and C. A. M. Afonso, *Chem. Eur. J.*, 2007, **13**, 8478; (b) N. M. M. Mateaus, L. C. Branco, N. M. T. Lopurenço and C. A. M. Afonso, *Green Chem.*, 2003, **5**, 347.
44. R. W. Johnson, *Tetrahedron Lett.*, 1976, **8**, 589.
45. A. M. O'Mahony, D. S. Silvester, L. Aldous, C. Hardacre and R. G. Compton, *J. Chem. Eng. Data*, 2008, **53**, 2884.
46. H. Matsumoto, M. Yanagida, K. Tanimoto, T. Kojima, Y. Tamiya and Y. Miyazaki, *Proc. Electrochem. Soc.: Molten Salts XII*, 2000, 186.
47. (a) C. D. Cowman, J. C. Thibeault, R. F. Ziolo and H. B. Gray, *J. Am. Chem. Soc.*, 1976, **98**, 3209; (b) R. Weiss, M. Rechinger and F. Hampel, *Zeit. Krist.*, 1995, **210**, 71; (c) H. N. Schaefer, H. Burzlaff, A. M. H. Grimmeiss, and R. Weiss, *Acta Cryst.*, 1992, **C48**, 795; (d) J. R. Butchard, O. J. Curnow, R. J. Pipal, W. T. Robinson and R. Shang, *J. Phys. Org. Chem.*, 2008, **21**, 127; (e) Alice T. Ku, M. Sundaralingam, *J. Am. Chem. Soc.*, 1972, **94**, 1688; (f) H. N. Schaefer, H. Burzlaff, A. M. H. Grimmeiss and R. Weiss, *Acta Cryst.*, 1992, **C48**, 912; (g) H. N. Schaefer, H. Burzlaff, A. M. H. Grimmeiss, R. Weiss, *Acta Cryst.*, 1991, **C47**, 1808.
48. (a) S. Wawzonek, W. McKillip and C. J. Peterson, *Org. Synth.*, 1964, **44**, 75; (b) J. J. Lucier, A. D. Harris and P. S. Korosec, *Org. Synth.*, 1964, **44**, 72.
49. O. V. Dolomanov, L. J. Bourhis, R. J. Gildea, J. A. K. Howard and H. Puschmann, *J. Appl. Cryst.*, 2009, **42**, 339.
50. G.M. Sheldrick, *Acta Cryst.*, 2008, **A64**, 112.

